CHAPTER-3

BACKGROUND OF MATERIAL MODELS

3.1 GENERAL

The material selection is very important when a structure is under high rate of loading and high temperature. The elastic damage model cannot define the proper behaviour of material under high impact load. When a RCC structure is subjected to high impact load due to an aircraft crash, the material behaviour is highly nonlinear.

Concrete properties change significantly in different complex loading environments (Ngo et al. 2007). It was found the strength of material under dynamic loading is higher than when the material is under static loading (Ngo et al. 2004). The strength of material is increased due to its viscosity and inertia effects also (Jiang and Chorzepa 2014). The % increase in tensile strength is higher than compressive strength, Lu and Xu (2004).

The concrete is a nonlinear material due its non-homogeneity. Tension and low compression failures can result in softening of the material. On the other hand, the high compression failures in concrete results in hardening of the material. In softening, the deformation increases with decreasing stress but in hardening, deformation increases with increasing stress. This phenomenon needs to be considered in consecutive model of concrete.

The behavior of concrete under compression and tension is totally different because it is a brittle material. The behaviour of concrete is more complex compared to steel reinforcement under high rate of loading. There are many material models are available in literature i.e., concrete brittle cracking model, concrete damaged plasticity model, concrete smeared cracking model, etc. It has been found that the concrete damaged plasticity (CDP) model is most appropriate model under impact loading.

To define the flow and fracture behavior of steel reinforcement under impact loading, a model was proposed by Johnson and Cook (J-C) in 1983 and 1985. The Johnson-Cook model is suitable for high rate of loading and very high temperature. This requires a simple method of calibration and less material parameters.

In the present study, CMP model for concrete, J-C material model for steel reinforcement and aircraft has also been considered. The degradation of modulus of elasticity and any other properties at elevated temperature has also been considered which has been taken from the recommendation of Eurocode 2.

3.2 CONCRETE MODEL UNDER IMPACT LOADING

To predict the nonlinear behavior and the damage of concrete structures under dynamic loading, the damaged plasticity model (DPM) for concrete in ABAQUS is used. This model can be used for PCC as well RCC structure. CDP model can also be used for monotonic, cyclic and dynamic loading. In conjunction with isotropic tensile and compressive plasticity, the model used the idea of isotropic damaged elasticity to reflect concrete's post-elastic behaviour.

Concrete behavior was employed using a damage plasticity model (DPM) available in ABAQUS / explicit manual because it has the ability to have the strain rate behavior. The material combines both the tension and compression of the concrete's plastic deformation. It was also believed that the material possibly will collapse under compression or tension-induced damages. This model can demonstrate the inelastic behavior of PCC and RCC concrete subject to static and dynamic loading. The nature of yield (or collapse) substances is regulated by two hardening factors, and related to compression and tension load failure mechanisms, respectively. The stress-strain nature of concrete generally shows a linear elastic relationship subjected to uniaxial tension until the failure stress (σ_{to}) is achieved. The variables of damage take values from 0-1, where '0' indicates undamaged material but '1' indicates complete loss in strength. The stress-strain curve for the concrete under tension and compression was shown in Fig. 3.1 (a) and 3.1 (b). The various damage parameters for stress-strain curve are given in the equation 3.1 and 3.2. The damage variables dt and dc is the function of the plastic strains, temperature, and field variables:

$$d_t = d_t\left(\tilde{\varepsilon}_t^{pl}, \theta, f_i\right)i \qquad 0 \le d_t \le 1$$

$$d_c = d_c\left(\tilde{\varepsilon}_c^{pl}, \theta, f_i\right)i \qquad 0 \le d_c \le 1$$

The damage parameters for concrete are defied as the below equations:

$$d_c = 1 - e^{-\alpha_c(\varepsilon_c - \varepsilon_{c0})/\varepsilon_{c0}} \ldots\ldots\ldots\ldots\ldots\ldots\ldots (3.1)$$

$$d_t = 1 - e^{-\alpha_t(\varepsilon_t - \varepsilon_{t0})/\varepsilon_{t0}} \ldots\ldots\ldots\ldots\ldots\ldots\ldots (3.2)$$

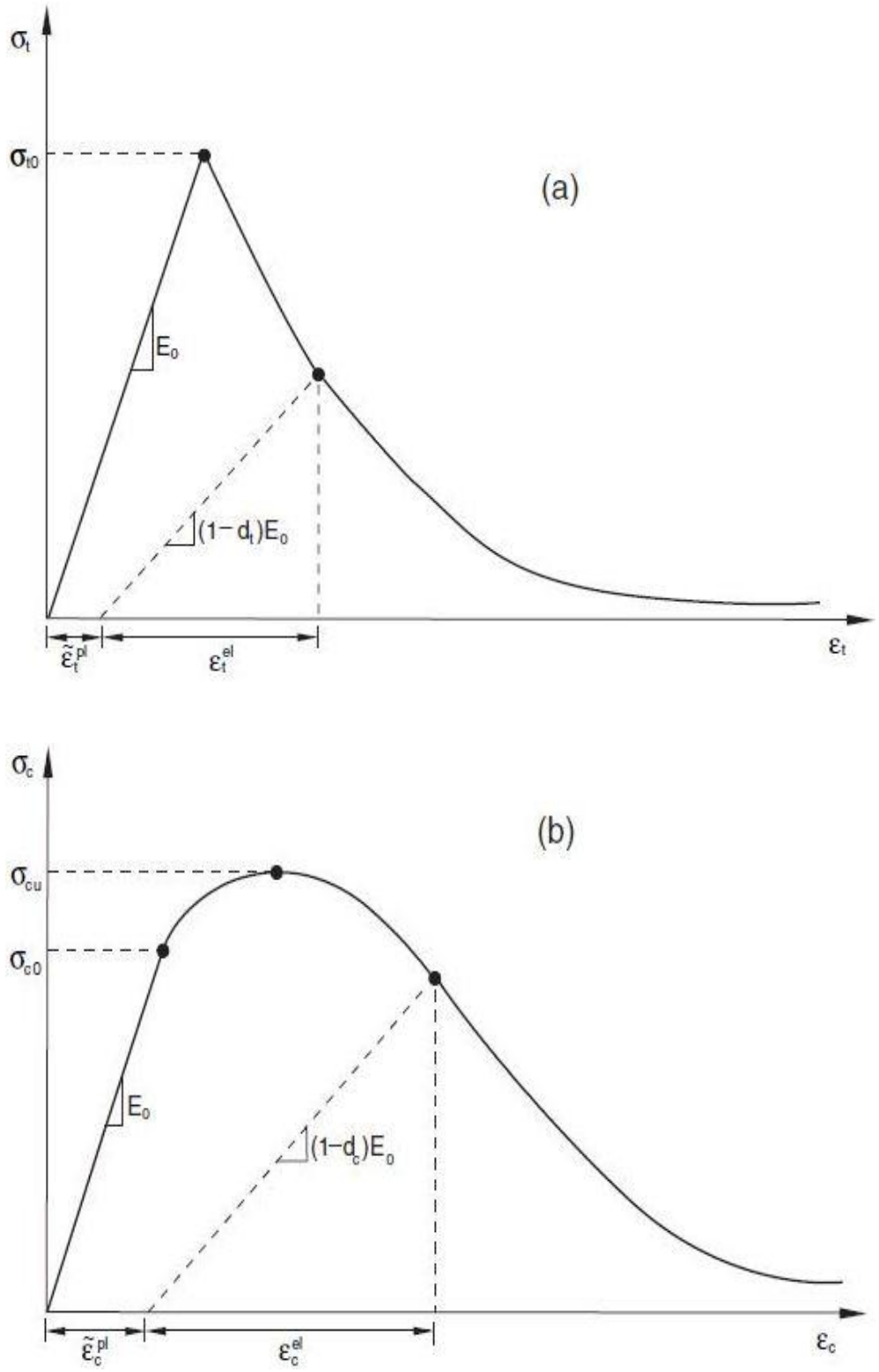

Fig. 3.1 Concrete Stress-strain curve (a) under tension (b) under compression

If the undamaged modulus of elasticity of concrete material is denoted by $E_{0,}$ then the stress-strain relations under tension and compression are:

$$\sigma_t = (1 - d_t)E_0\left(\varepsilon_t - \tilde{\varepsilon}_t^{pl}\right) \ldots\ldots\ldots\ldots\ldots\ldots (3.3)$$

$$\sigma_c = (1 - d_c)E_0\left(\varepsilon_c - \tilde{\varepsilon}_c^{pl}\right) \ldots\ldots\ldots\ldots\ldots\ldots (3.4)$$

In terms of a scalar degradation variable, the CDP model assumes that the reduction of the elastic modulus is given as

$$E = (1 - d)\, E_0 \ldots\ldots\ldots\ldots\ldots\ldots\ldots (3.5)$$

Where:

d_t, d_c	Damages parameter (values vary from zero to one)
$\tilde{\varepsilon}_c^{pl}$	Compressive plastic strain
$\tilde{\varepsilon}_t^{pl}$	Tensile plastic strain
E_0	Initial elastic stiffness (undamaged)
$\tilde{\varepsilon}_t^{el}$	Tensile elastic strain
$\tilde{\varepsilon}_c^{el}$	Compressive elastic strain
$\alpha_{c,}\ \alpha_t$	damage parameters
ε_{c0}	compressive strain corresponding to peak compressive stress
ε_{t0}	Tensile strain corresponding to peak tensile stress

Tension stiffening is modelled on the post-failure behavior of direct strain, which helps to describe the strain-softening behavior of cracked concrete. This activity also makes it possible to simulate in a simple way the results of the reinforcement contact with concrete. The CDP model includes tension stiffening.

The post failure behaviour of concrete under tensile load is a function of cracking

strain, $\tilde{\varepsilon}_t^{ck}$. The total strain minus the elastic strain is known as the cracking strain and that is $\tilde{\varepsilon}_t^{ck} = \varepsilon_t - \varepsilon_{0t}^{el}$, where $\varepsilon_{0t}^{el} = {}^{\sigma_t}/_{E_0}$, shown in Fig. 3.2.

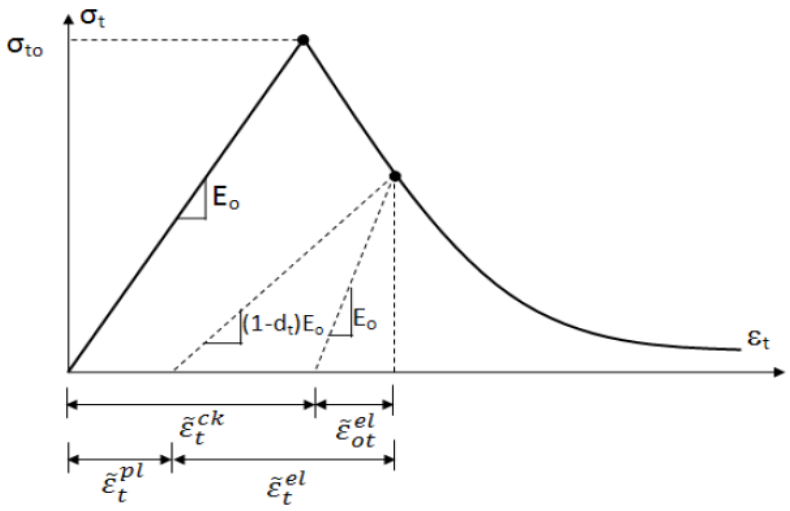

Fig. 3.2 Cracking strain under tension stiffening

The concrete material gets cracked when the deformation is beyond the permissible deformation. This phenomenon is used by fracture energy concept. The fracture energy vs deformation curve has been shown in Fig. 3.3. In the present study, the concrete brittle fracture criterion (using stress-displacement response) was incorporated in the material properties to define the target damage.

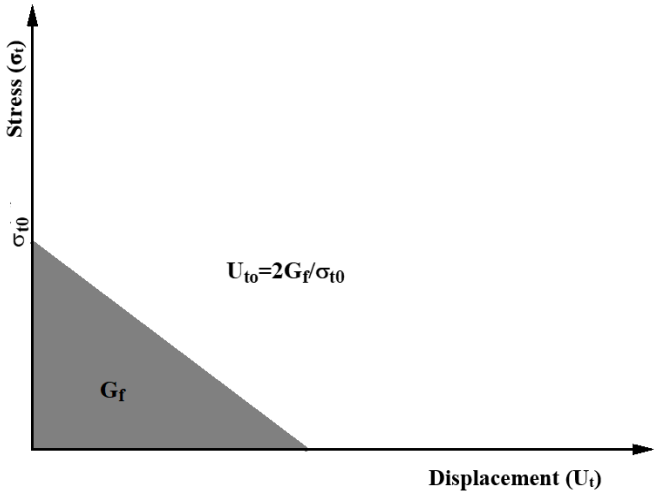

Fig. 3.3 Fracture energy curve after failure

Hillerborg (1976) used the brittle fracture concept to define the energy required to open a unit area of crack, Gf, as a material parameter. The cracking displacement can be calculated by $u_{t0} = 2G_f/\sigma_{t0}$. The range of G_f vary from 40 N/m to 120 N/m. For normal concrete, the value of G_f is 40N/m whereas for high concrete the value is 120N/m. (for M40 concrete).

The total strain minus the elastic strain corresponding to the undamaged material is known as the compressive inelastic strain, $\tilde{\varepsilon}_c^{in} = \varepsilon_c - \varepsilon_{0c}^{el}$ and $\varepsilon_{0c}^{el} = {\sigma_c}/{E_0}$, shown in Fig. 3.4 and Fig. 3.5.

Using the below relationship, Abaqus automatically transforms inelastic strain values to plastic strain values.

$$\tilde{\varepsilon}_c^{pl} = \tilde{\varepsilon}_c^{in} - \frac{d_c}{(1-d_c)}\frac{\sigma_c}{E_0} \dots\dots\dots\dots\dots\dots\dots (3.6)$$

The plastic and inelastic strain is same when the damages parameter is not taken in Damage Plasticity Model (DPM). In my research, the behavior of concrete under compression with different strain rate has been considered from the work of Grote et al., 2001 and Sinha et al., 1964. Sinha et al. performed cyclic loading tests on cylinders with quite low strain value whereas Grote et al. performed experiments at different strain rates (290 s^{-1}, 620 s^{-1}, 1050 s^{-1}, 1500 s^{-1}) which has been shown in Fig. 3.6 and Fig. 3.7 respectively. Total five curves were used in DPM for compression behavior.

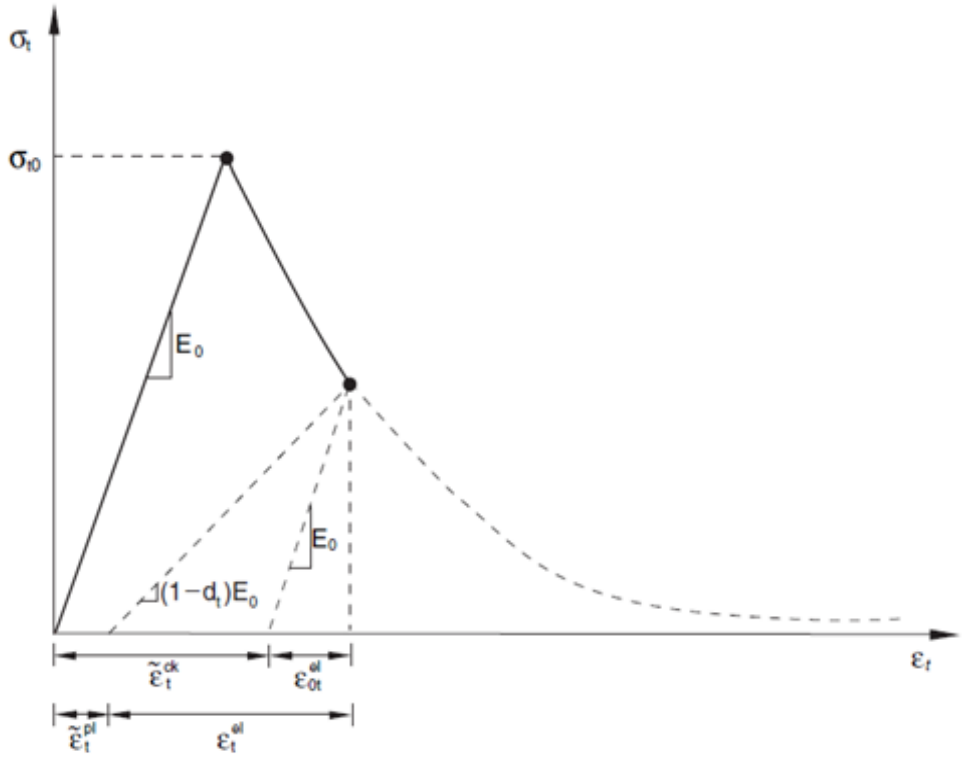

Fig. 3.4 Cracking tensile strain in compression hardening

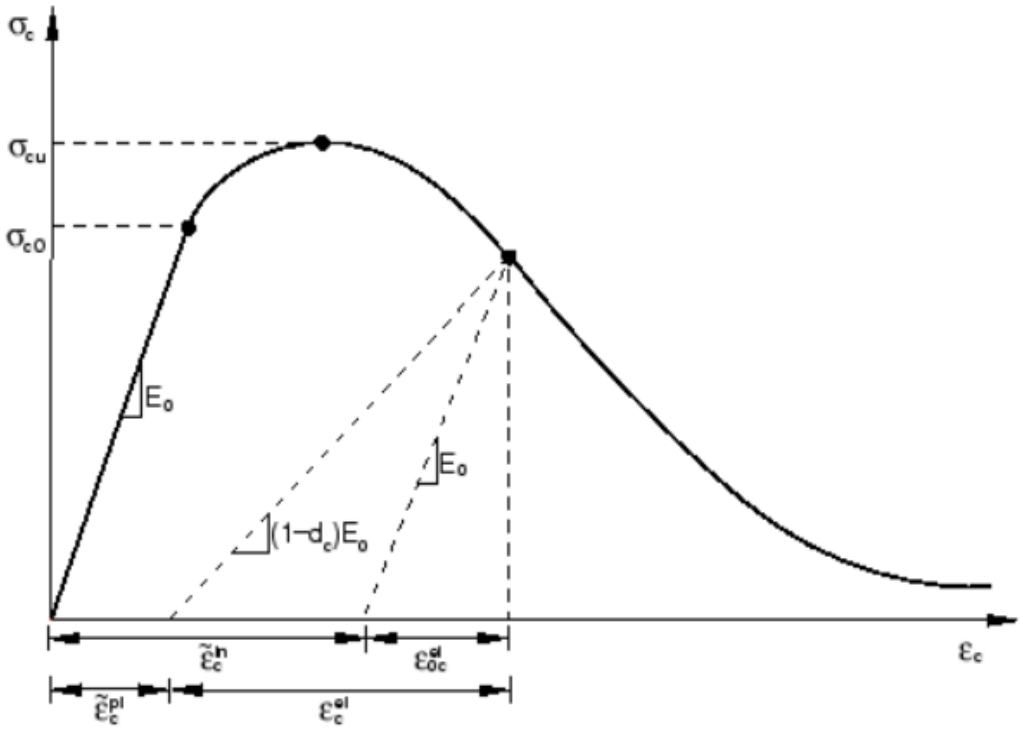

Fig. 3.5 Compressive inelastic strain in compression hardening

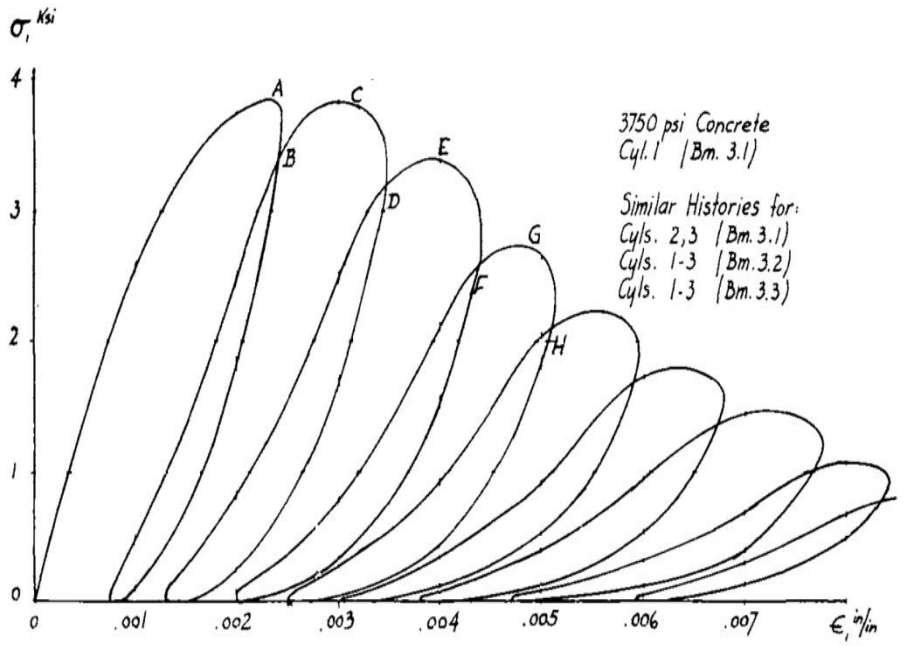

Fig. 3.6 Concrete bevaviour with cyclic loading (Sinha et al. 1964)

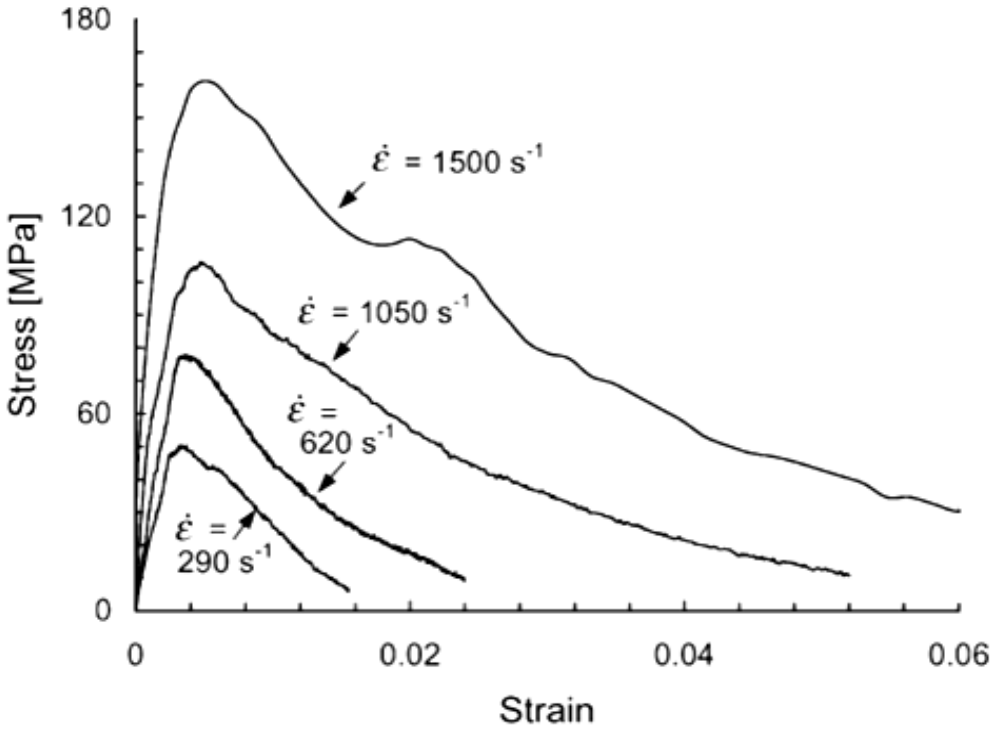

Fig. 3.7 Concrete bevaviour with different strain rate under compression (Grote et al.,2001)

The behavior of concrete subjected to tension with different strain rate (20 s^{-1}, 80 s^{-1}, 160 s^{-1}) has been considered from the work of Lu and Xu (2004), Fig. 3.8. Fig. 3.9 and Fig. 3.10 demonstrate the variance of the dynamic to static strength ratio with strain rate under compressive and tensile loading. The increase in dynamic concrete tensile strength has been found to be much higher than that of dynamic compressive strength. Figure 3.11 also indicates an increase in the fracture energy of concrete, with an increase in the strain rate. The parameters related to Damage Plasticity Model has been given in Table 3.1. The viscosity parameter is generally used when rate dependent analysis is conducted. The dilation angle defines amount of plastic volumetric strain induced in plastic shear. The flow potential eccentricity in the stress-strain relation shows the rate at which the function approaches asymptote in the hyperbolic surface of plastic potential in meridional plane. The K parameter controls how the yield surface will shape like.

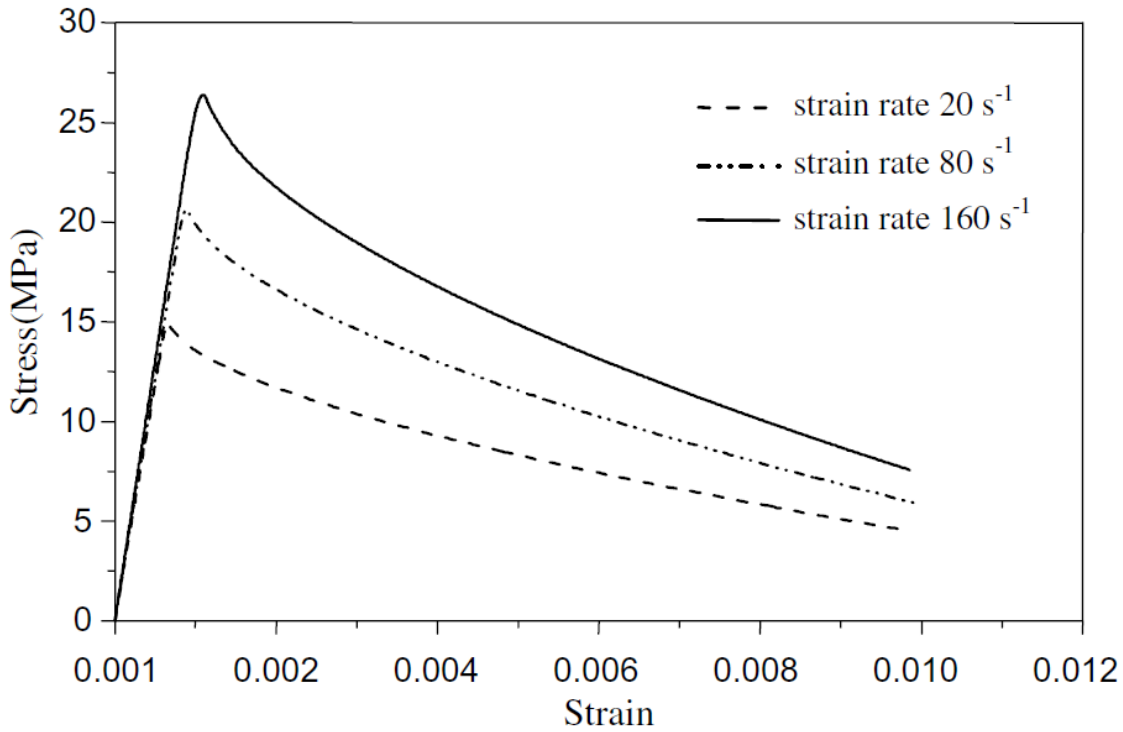

Fig. 3.8 Stress-strain curves for concrete for different strain rates under tensile loading (Lu and Xu, 2004)

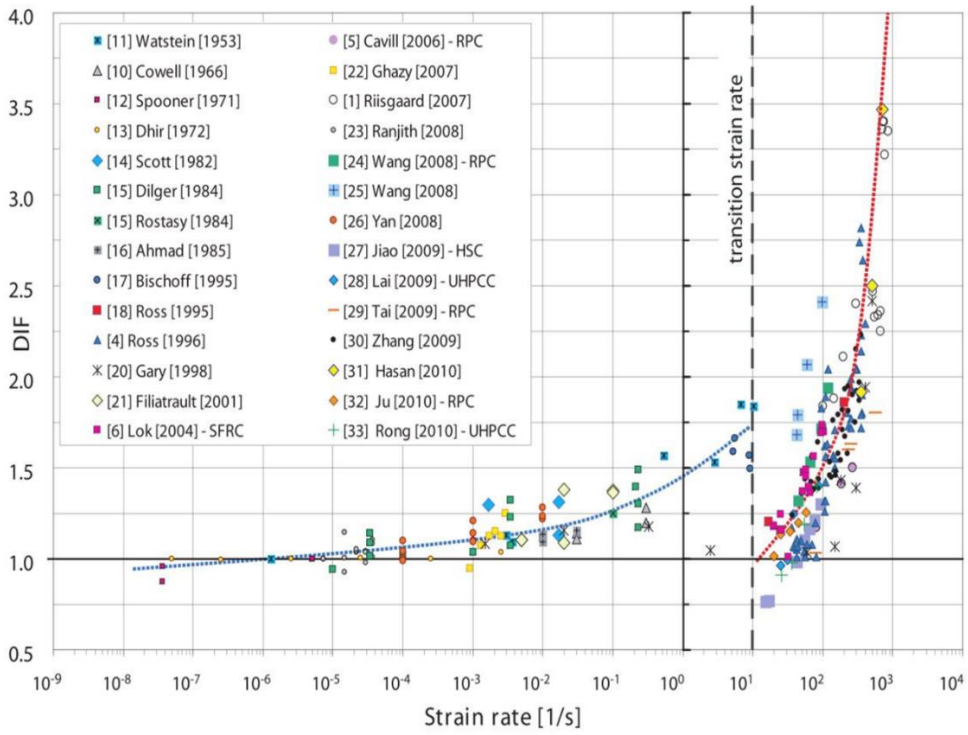

Fig. 3.9 Dynamic increase factor (DIF) of concrete with different strain rate (Pajak M., 2011)

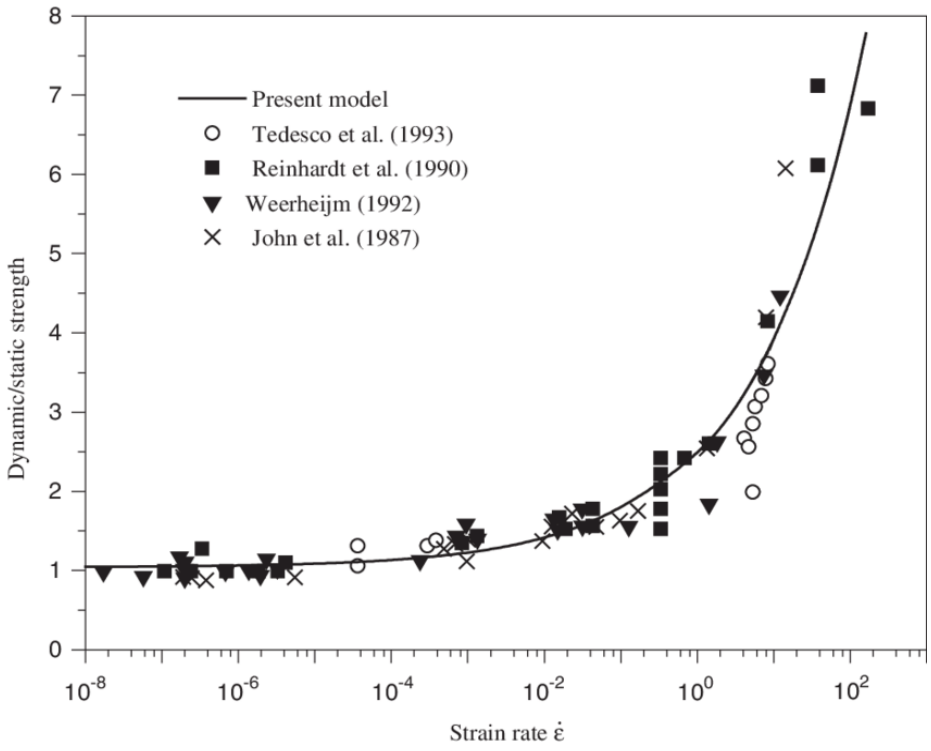

Fig. 3.10 Normalized concrete tensile strength vs strain rate (Lu and Xu, 2006)

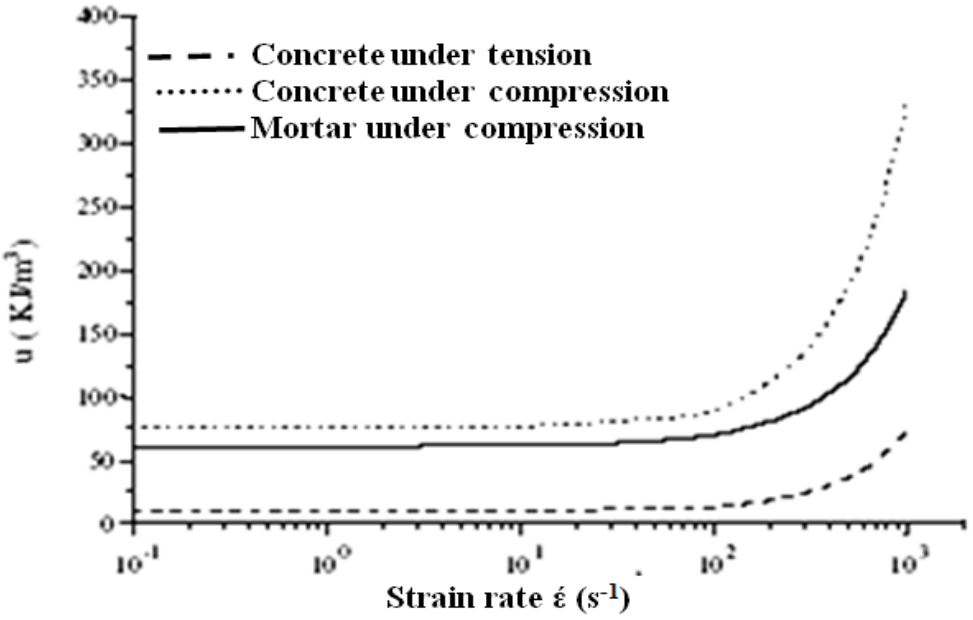

Fig. 3.11 Variation of fracture energy with strain rate

Table 3.1 Concrete properties (DPM Parameters)

Density (kg/m^3)	2400
Poisson's ratio	0.17
Elastic modulus (N/m^2)	2.7x10^{10}
Fracture Energy (N/m)	720
Compressive Strength (Pa)	30 x 10^6
Dilation angle	30
Eccentricity	1.0
Failure stress in tension (N/mm^2)	10.8
Compressive Strength (N/mm^2)	30
K (the ratio of the second stress invariant on the tensile meridian to that on the compressive meridian)	0.667

3.3 CONCRETE MODEL UNDER FIRE

Concrete behavior is really different in ambient and elevated temperature. The fire may damage both the properties of concrete mechanical as well as chemical when the temperature is very high. In this simulation, the properties of concrete and stress-strain behaviour at very high temperature should be taken carefully. In present study the concrete properties (modulus of elasticity, specific heat, conductivity, thermal expansion, strength) have been used with the help of Euro-code 2, 2004. The stress-strain curve of concrete at varying temperature has been drawn with the help of Fig. 3.12 and Table 3.2. The relation between stress-strain is made up of two variables i.e., stress $f_{c,\theta}$ and strain $\varepsilon_{c1,\theta}$. Using Table 3, the stress-strain curves for M30 concrete at different temperature under compression has been plotted and shown in Fig. 3.13.

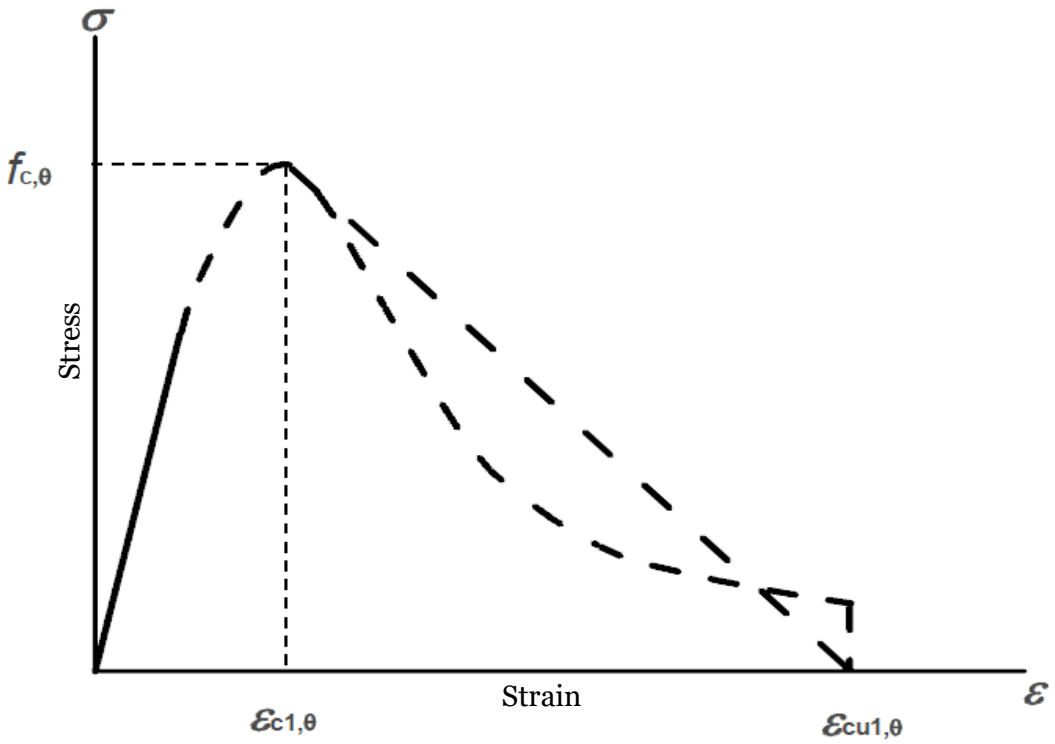

Fig. 3.12 Concrete with varying temperature under compression (Eurocode 2)

Table 3.2 Concrete Stress-strain behavior at varying temperatures (Euro-code 2)

Range	$\varepsilon \leq \varepsilon_{c1,\theta}$	$\varepsilon_{c1(\theta)} < \varepsilon \leq \varepsilon_{cu1,\theta}$
Stress σ	$\frac{3\varepsilon f_{c,\theta}}{\varepsilon_{c1,\theta}\left(2+\left(\frac{\varepsilon}{\varepsilon_{c1,\theta}}\right)^{3}\right)}$	Linear models for numerical purposes

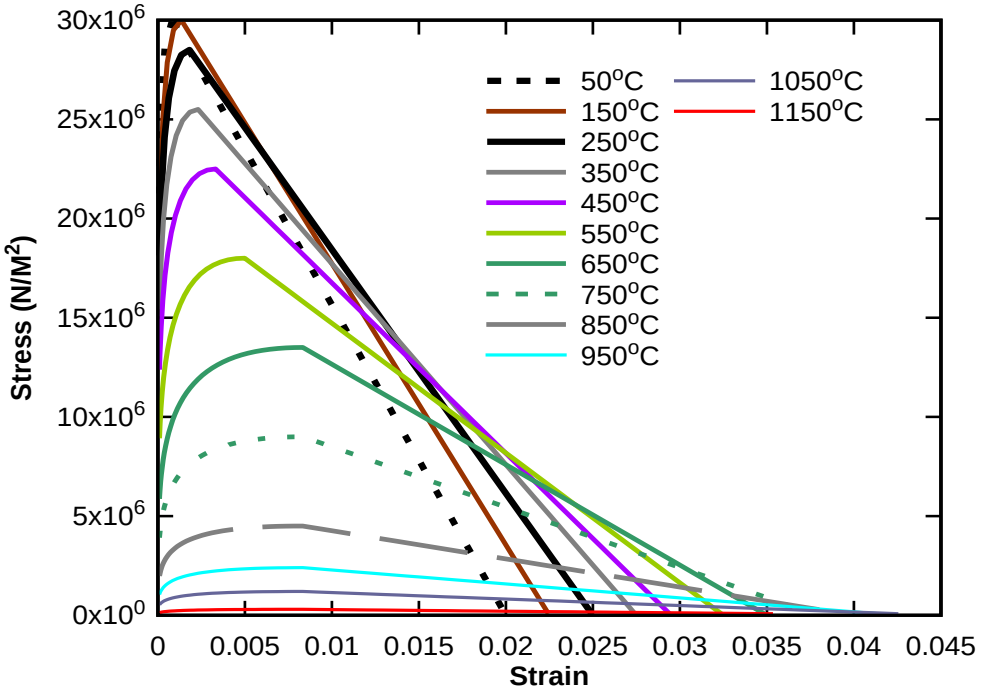

Fig. 3.13 Stress-strain plot at different temperature

The value of parameter in stress-strain formula is depending upon the types of aggregate used in concrete and temperature. The aggregate may be siliceous or calcareous in nature. The value of parameter for both the aggregate under different temperatures is given in Table 3.3.

Table 3.3 The parameters used in stress-strain relationships (Eurocode-2)

Temp. ^{o}C	Siliceous aggregate			Calcareous aggregate		
^{o}C	$f_{c,\theta} / f_{ck}$	$\varepsilon_{c1,\theta}$	$\varepsilon_{cu1,\theta}$	$f_{c,\theta} / f_{ck}$	$\varepsilon_{c1,\theta}$	$\varepsilon_{cu1,\theta}$
20	1.00	0.0025	0.0200	1.00	0.0025	0.0200
100	1.00	0.0040	0.0225	1.00	0.0040	0.0225
200	0.95	0.0055	0.0250	0.97	0.0055	0.0250
300	0.85	0.0070	0.0275	0.91	0.0070	0.0275
400	0.75	0.0100	0.0300	0.85	0.0100	0.0300
500	0.60	0.0150	0.0325	0.74	0.0150	0.0325
600	0.45	0.0250	0.0350	0.60	0.0250	0.0350
700	0.30	0.0250	0.0375	0.43	0.0250	0.0375
800	0.15	0.0250	0.0400	0.27	0.0250	0.0400
900	0.08	0.0250	0.0425	0.15	0.0250	0.0425
1000	0.04	0.0250	0.0450	0.06	0.0250	0.0450
1100	0.01	0.0250	0.0475	0.02	0.0250	0.0475
1200	0.00	-	-	0.00	-	-

With the increase in temperature, the modulus of elasticity decreases quickly which is shown in Figure 3.14. The modulus of elasticity under elevated temperature has also been plotted using Eurocode-2.

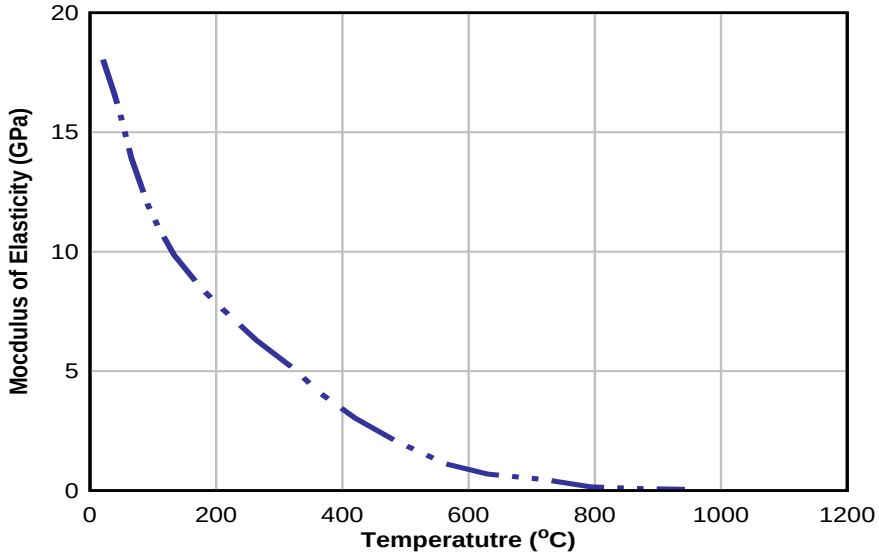

Fig. 3.14 Youngs modulus of the concrete with varying temperature

Thermal conductivity, thermal expansion and specific heat of concrete material is also influenced by high temperature. So, this behavior should be incorporated in the material model. The Fig. 3.15, 3.16 and 3.17 are showing the variation of thermal conductivity, thermal expansion and specific heat at varying temperature respectively. With the help of some formulations which are exist in Eurocode 2, 2004, these plots have been drawn.

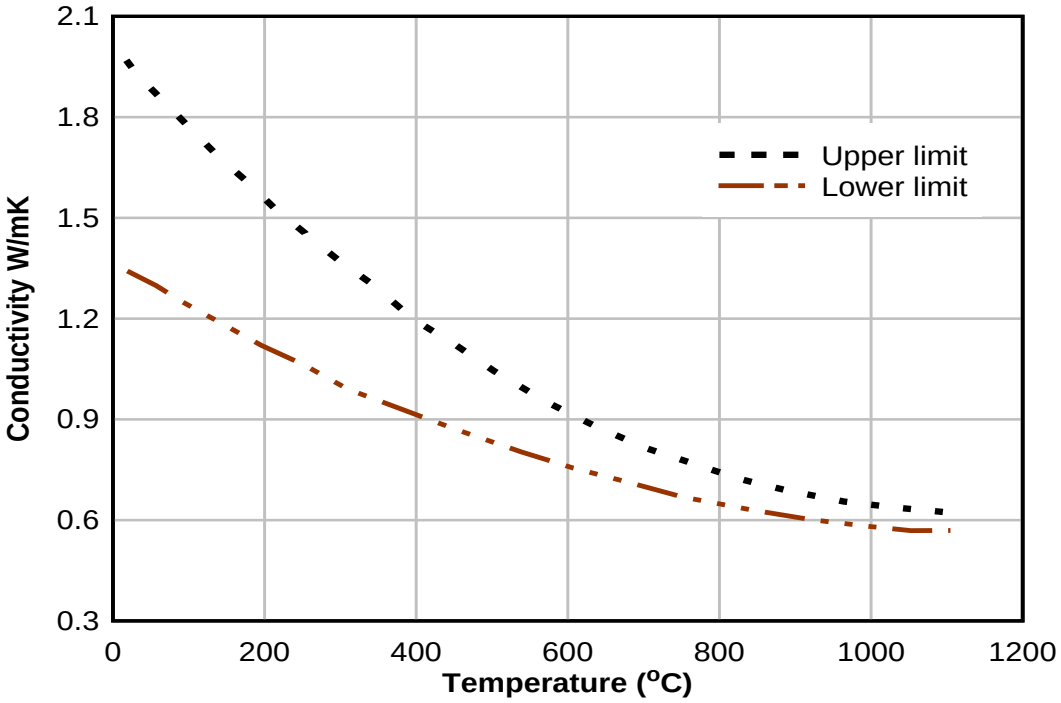

Fig. 3.15 Thermal conductivity of concrete with varying temperature

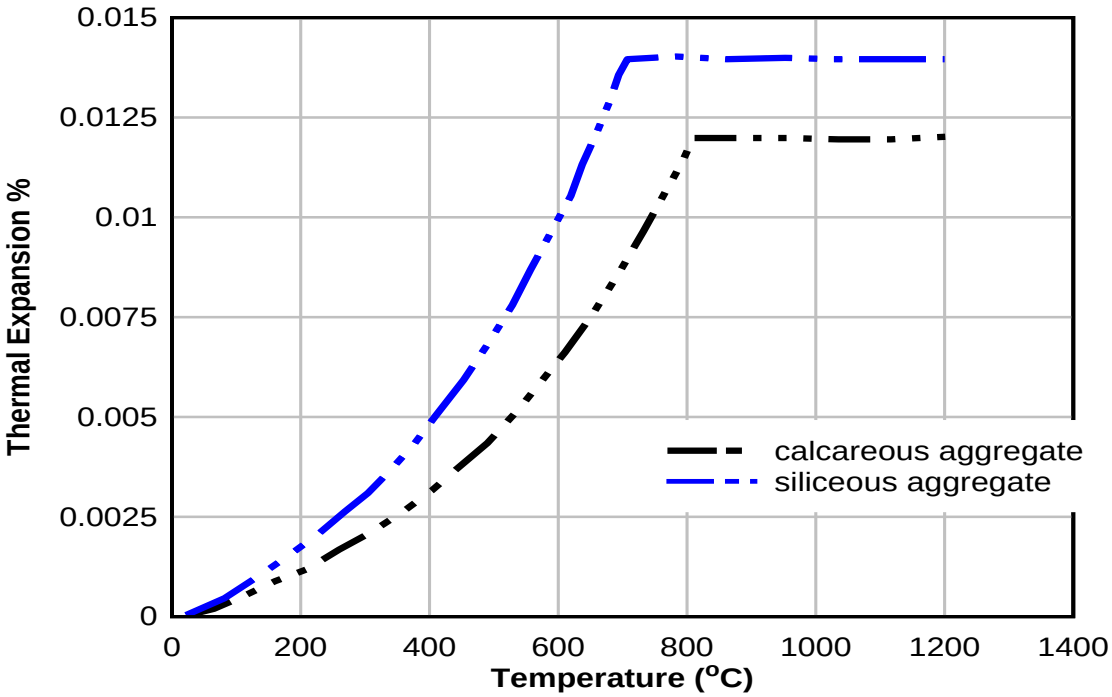

Fig. 3.16 Expansion coefficient with varying temperature

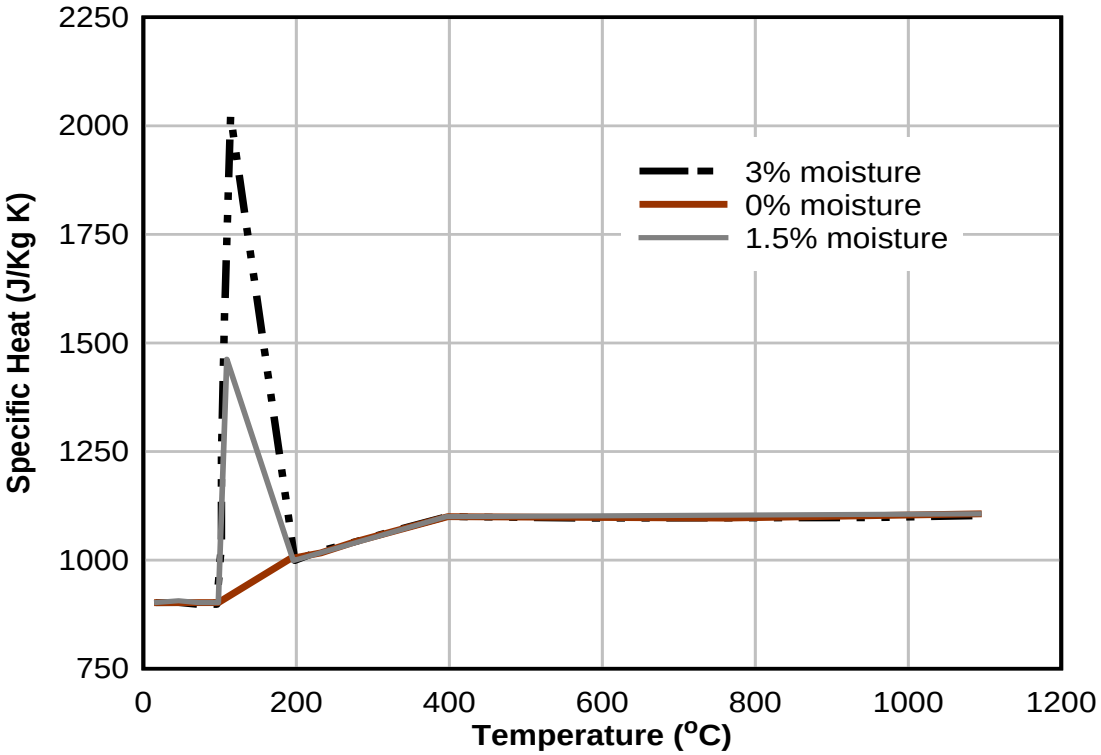

Fig. 3.17 Specific heat concrete with temperature

3.4 REINFORCEMENT MODEL UNDER IMPACT LOADING AND FIRE

The reinforcement steel bar behavior was implemented using the very popular Johnson-Cook material model which has the ability to predict fracture of ductile materials. The Johnson-Cook model's effect of strain hardening, stress rate, and temperature is described in the following way in equation 3.7 and 3.8. The parameters related to Johnson Cook model has given in Table 3.4 (Murugesan M. and Jung D. W., 2019). The Johnson-Cook fracture model has three independent parts (stress, strain rate and temperature) to give the actual behaviour of reinforcement bar which has been given equation 3.9.

$$\overline{\sigma}(\bar{\varepsilon}^{pl}, \dot{\bar{\varepsilon}}^{pl}, \hat{T}) = \left[A + B(\bar{\varepsilon}^{pl})^{n}\right]\left[1 + C\ln\left(\frac{\dot{\bar{\varepsilon}}^{pl}}{\dot{\varepsilon}_0}\right)\right]\left[1 - \hat{T}^{m}\right] \text{----------(3.7)}$$

$$\hat{T} = (T - T_0)/(T_{melt} - T_0) \qquad T_0 \le T \le T_{melt} \text{----------(3.8)}$$

$$\bar{\varepsilon}^{pl}{}_{f}\left(\frac{\sigma_m}{\bar{\sigma}}, \dot{\bar{\varepsilon}}^{pl}, \hat{T}\right) = \left[D_1 + D_2\exp\left(D_3\frac{\sigma_m}{\bar{\sigma}}\right)\right]\left[1 + D_4\ln\left(\frac{\dot{\bar{\varepsilon}}^{pl}}{\dot{\varepsilon}_0}\right)\right]\left[1 + D_5\hat{T}\right] \text{----------}$$

(3.9)

Where:

$\overline{\sigma}$	Equivalent von Mises stress
$\hat{T}$	Non-dimensional temperature
$\dot{\varepsilon}_0$	Reference strain rate
$\dot{\bar{\varepsilon}}^{pl}$	Rate of equivalent plastic strain
$\bar{\varepsilon}^{pl}$	Equivalent plastic strain
A, B, C, n and m	Material constants

T_0	Reference temperature
T	Deformation temperature
T_{melt}	Melting temperature
D_1, D_2, D_3, D_4, D_5	Damage constants
$\frac{\sigma_m}{\overline{\sigma}}$	Ratio between mean stress and equivalent stress

Table 3.4 Properties of reinforcement and Johnson-Cook Parameters (Murugesan M. and Jung D. W., 2019)

Density (Kg/m^3)	7850	T_{melt} (Kelvin)	1800
Young's modulus (N/m^2)	2 x10^{11}	T_0 (Kelvin)	293
Poisson Ratio	0.33	Cp (J/ Kg K)	452
A (N/m^2)	49 x 10^7	α	0.9
B (N/ m^2)	38.3 x 10^7	D1	0.0705
n	0.45	D2	1.732
$\dot{\varepsilon}$ (s^{-1})	5x10^{-4}	D3	-0.54
C	0.0114	D4	-0.01
m	0.94	D5	0.0

At varying temperatures, Euro-code 2 provides the deformation and strength properties of reinforcement steel bar. Fig. 3.18 shows the stress-strain relationship at different temperatures and which has been taken from Euro-code 2. With the help of Table 3.5, the stress-strain plots for several elevated temperatures have been drawn (Fig. 3.19).

Table 3.5 Mathematical equation for stress-strain curves of steel rebar at different temperatures

Range	$\varepsilon_{sp,\theta}$	$\varepsilon_{sp,\theta} \leq \varepsilon \leq \varepsilon_{sy,\theta}$	$\varepsilon_{sy,\theta} \leq \varepsilon \leq \varepsilon_{st,\theta}$	$\varepsilon_{st,\theta} \leq \varepsilon \leq \varepsilon_{su,\theta}$	$\varepsilon = \varepsilon_{su,\theta}$
Stress σ	$\varepsilon E_{s,\theta}$	$f_{sp,\theta} - c+(b/a)\left[a^2 - \left(\varepsilon_{sy,\theta} - \varepsilon\right)^2\right]^{0.5}$	$f_{sy,\theta}$	$f_{sy,\theta}\left[1 - \left(\varepsilon - \varepsilon_{st,\theta}\right)\Big/\left(\varepsilon_{su,\theta} - \varepsilon_{st,\theta}\right.\right.$	0.00
Modulus of Tangent	$\varepsilon E_{s,\theta}$	$\frac{b(\varepsilon_{sy,\theta} - \varepsilon)}{a\left[a^2 - \left(\varepsilon - \varepsilon_{sy,\theta}\right)^2\right]^0}$	0	--	--
Functions	$c = \frac{(f_{sy,\theta} - f_{sp,\theta})^2}{(\varepsilon_{sy,\theta} - \varepsilon_{sp,\theta})E_{s,\theta} - 2(f_{sy,\theta} - f_{sp,\theta})}$ $a^2 = (\varepsilon_{sy,\theta} - \varepsilon_{sp,\theta})(\varepsilon_{sy,\theta} - \varepsilon_{sp,\theta} + c/E_{s,\theta})$ $b^2 = c\,(\varepsilon_{sy,\theta} - \varepsilon_{sp,\theta})E_{s,\theta}$				
Parameters	$\varepsilon_{su,\theta} = 0.20$	$\varepsilon_{st,\theta} = 0.15$	$\varepsilon_{sp,\theta} = \frac{f_{sp,\theta}}{E_{s,\theta}}$	$\varepsilon_{sy,\theta} =$ 0.02	

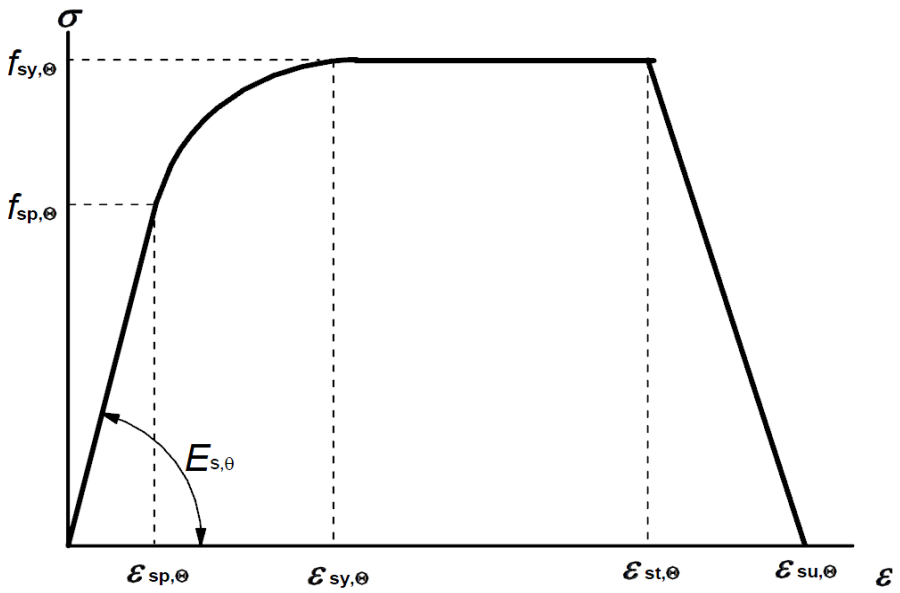

Fig. 3.18 Stress-strain curve of steel bar at elevated temperatures (Eurocode-2)

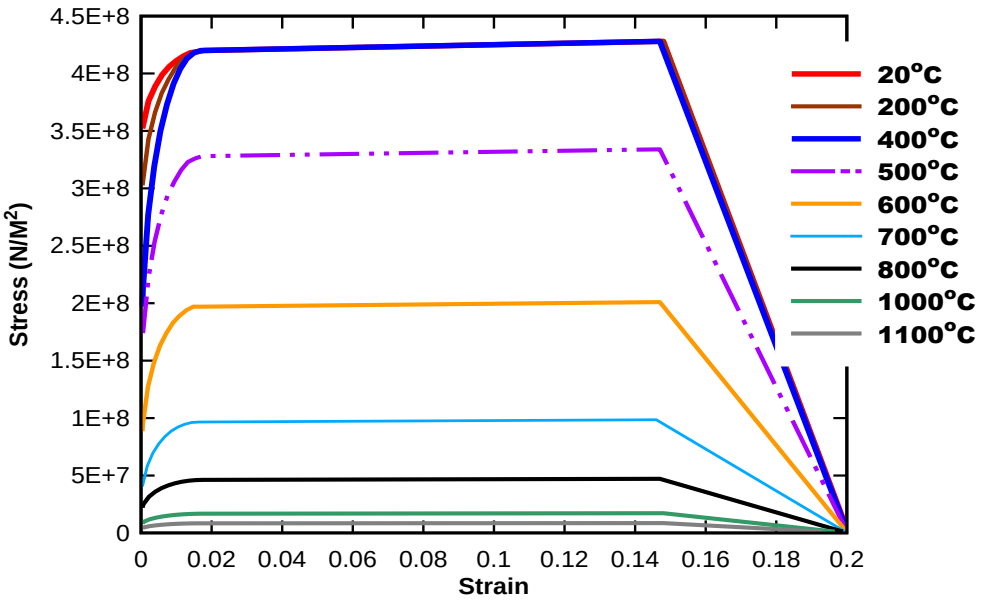

Fig. 3.19 Stress-strain plots of steel at different temperatures

3.5 MATERIAL PROPERTIES FOR AIRCRAFT MODEL

It is quite complex and difficult to create an exact dimensionally symmetric model of each and every aircraft. Starke Jr. and Staley Jr. provided a detailed overview of the

various aircraft structure components and the related aluminium alloys. (1996). The main components of the Boeing 707-320 body are made up of aluminum alloy Al 7178-T6511. The properties of Al 7178-T651 have been shown in Table 3.6.

Table 3.6 The properties for Aluminum alloy Al 7178-T651

Yield stress, A (N/m^2)	$4.3e^8$
Poisson Ratio, ϑ	0.33
Density,ρ (kg/m^3)	2795
Young's modulus; E (N/ m^2)	$7.10X\ 10^{10}$